Maximum Likelihood Method for MIMO Mobile-to-mobile Channel Parameter Estimation

Alenka G. Zajić and Gordon L. Stüber
School of Electrical and Computer Engineering
Georgia Institute of Technology, Atlanta, GA 30332 USA

***Abstract*— A three-dimensional reference model for wideband multiple-input multiple-output mobile-to-mobile channels is reviewed. To allow comparison between the proposed model and measured data, a new maximum likelihood based stochastic estimator is derived. The proposed estimator extracts the relevant model parameters from the measured data. The performance of the new estimator is evaluated by deriving the Cramér-Rao lower bound (CRLB) and by comparing the mean square error of the parameter estimates to the CRLB. Simulation results show that the proposed estimator has an asymptotically optimal performance, since it reaches the CRLB for a small number of samples.**

I. Introduction

Mobile-to-mobile (M-to-M) communications play an important role in mobile ad-hoc wireless networks, intelligent transportation systems, and relay-based cellular networks. The statistical properties of M-to-M channels are quite different from conventional fixed-to-mobile (F-to-M) cellular land mobile radio channels [1]. M-to-M communication systems are equipped with low elevation antennas and have both the transmitter and receiver in motion. Akki and Haber [1] proposed a two-dimensional (2-D) reference model for single-input single-output (SISO) M-to-M Rayleigh fading channels. Reference models for 2-D narrowband multiple-input multiple-output (MIMO) M-to-M channels have been proposed in [2], [3]. To appropriately model an urban environment, we have recently proposed the three-dimensional (3-D) reference model for *narrowband* and *wideband* MIMO M-to-M multipath fading channels [4], [5].

Realistic M-to-M channel models are necessary for successful design of M-to-M systems. In order to validate channel models, comparison between the channel models and measurements, and consequently estimation of the model parameters, is necessary. Deterministic parameter estimation techniques employ deterministic channel models that have a large number of discrete waves with unknown amplitudes, phases, and frequencies (e.g., Space Alternating Generalized Expectation-maximization (SAGE) algorithm) [6], [7]. Such an estimation approach leads to maximization of highly non-linear likelihood functions with many local optima, which causes convergence problems [8]. On the other hand, stochastic channel parameter estimation techniques employ statistical channel models, where the only unknowns are the parameters of the distribution functions used to characterize the angles of departure and the angles of arrival. The first stochastic estimator, which employs the 2-D MIMO F-to-M channel model in [9] and estimates the parameters in the von Mises distribution function, is introduced in [10]. Compared to the deterministic parameter estimation approach, this method leads to lower complexity and faster convergence [11], [12].

In this paper, a new maximum likelihood based stochastic estimator is derived to extract the parameters needed for our 3-D wideband MIMO M-to-M channel reference model in [5] from measured data. The new estimator jointly estimates the parameters of the distribution functions used to characterize the azimuth and elevation angles of departure, the azimuth and elevation angles of arrival, and the parameters that specify how much the single- and double-bounced rays contribute to the total averaged received power. This estimator is an extension of the stochastic estimator in [10], which only estimates the parameters of the distribution function used to characterize the azimuth angles of arrival. The performance of the new estimator is evaluated by deriving the Cramér-Rao lower bound (CRLB) and by comparing the mean square error of the parameter estimates to the CRLB. Simulation results show that the proposed estimator has an asymptotically optimal performance, since it reaches the CRLB for a small number of samples.

The remainder of the paper is organized as follows. For ease of reference, Section II reviews our 3-D wide-band MIMO M-to-M reference model and its space-time-frequency correlation function (STF-CF). Section III presents the new maximum likelihood based stochastic estimator. Section IV derives the CRLB for the proposed estimator. Section V compares the mean square error of the parameter estimates to the CRLB and evaluates the performance of the proposed estimator by comparing the analytical and measured STF-CF. Finally, Section VI provides some concluding remarks.

II. A 3-D Theoretical Model for Wideband MIMO Mobile-to-Mobile Channels

This section reviews our 3-D theoretical model for wideband MIMO M-to-M multipath fading channels proposed in [5]. We consider a wideband MIMO communication system with L_t transmit and L_r receive omnidirectional antenna elements. It is

0 Prepared through collaborative participation in the Collaborative Technology Alliance for Communications & Networks sponsored by the U.S. Army Research Laboratory under Cooperative Agreement DAAD19-01-2-0011. The U.S. Government is authorized to reproduce and distribute reprints for Government purposes notwithstanding any copyright notation thereon.

assumed that both the $\mathrm{T_x}$ and $\mathrm{R_x}$ are in motion and equipped with low elevation antennas. The radio propagation occurs in outdoor metropolitan environments that are characterized by 3-D non-isotropic scattering with either line-of-sight (LoS) or non-line-of-sight (NLoS) conditions between the $\mathrm{T_x}$ and $\mathrm{R_x}$. The MIMO channel can be described by an $L_r \times L_t$ matrix $\mathbf{T}(t,f) = [T_{ij}(t,f)]_{L_r \times L_t}$ of the time-variant transfer functions.

The 3-D reference model is derived using the 3-D geometrical "concentric-cylinders" model shown in Fig. 1. Around the $\mathrm{T_x}$, M fixed omnidirectional scatterers occupy a volume between cylinders of radii R_{t1} and R_{t2}. It is assumed that the M scatterers lie on L cylindric surfaces of radii $R_{t1} \le R_t^{(l)} \le R_{t2}$, where $1 \le l \le L$. The l^{th} cylindric surface contains $M^{(l)}$ fixed omnidirectional scatterers, and the $(m,l)^{th}$ transmit scatterer is denoted by $S_T^{(m,l)}$, where $1 \le m \le M^{(l)}$. Similarly, around the $\mathrm{R_x}$, N fixed omnidirectional scatterers occupy a volume between cylinders of radii R_{r1} and R_{r2}. It is assumed that the N scatterers lie on P cylindric surfaces of radii $R_{r1} \le R_r^{(k)} \le R_{r2}$, where $1 \le k \le P$. The k^{th} cylindric surface contains $N^{(k)}$ fixed omnidirectional scatterers, and the $(n,k)^{th}$ receive scatterer is denoted by $S_R^{(n,k)}$, where $1 \le m \le N^{(k)}$. The parameters in Fig. 1 are defined in Table I.

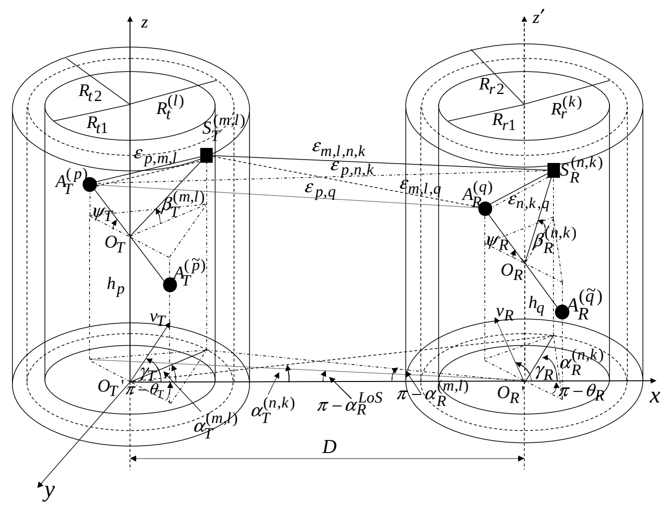

Fig. 1. The "concentric-cylinders" model with LoS, single-bounced transmit, single-bounced receive, and double-bounced rays for a MIMO M-to-M channel with $L_t = L_r = 2$ antenna elements.

The time-variant transfer function of the link $A_T^{(p)}$ - $A_R^{(q)}$ is defined as a superposition of the LoS, single-bounced transmit, single-bounced receive, and double-bounced rays [5]

$$T_{pq}(t,f) = T_{pq}^{LoS}(t,f) + T_{pq}^{SBT}(t,f) + T_{pq}^{SBR}(t,f) + T_{pq}^{DB}(t,f), \quad (1)$$

where the single-bounced transmit, single-bounced receive, double-bounced, and LoS components of the time-variant transfer function are defined in (3), (4), (8), (11) of [5], respectively.

The model in [5] assumes that the angles of departure and the angles of arrival are random variables. The azimuth angles of departure and arrival, $\alpha_T^{(m,l)}$ and $\alpha_R^{(n,k)}$, are characterized by the von Mises probability density function (pdf) [13]. The elevation angles of departure and arrival, $\beta_T^{(m,l)}$ and $\beta_R^{(n,k)}$, are characterized by the pdf [14] $f(\varphi) = \pi\cos\left(\pi\varphi/(4\varphi_m)\right)/(4|\varphi_m|)$ for $|\ \varphi\ | \le |\ \varphi_m\ | \le \pi/2$ and $f(\varphi) = 0$ otherwise. The parameter φ_m is the maximum elevation angle and lies in the range $0^\circ \le |\ \varphi_m\ | \le 20^\circ$ [5]. Finally, the radii $R_t^{(l)}$ and $R_r^{(k)}$ are characterized by the pdf $f(R) = 2R/(R_2^2 - R_1^2)$ [5].

The normalized STF-CF between two time-variant transfer functions $T_{pq}(t,f)$ and $T_{\tilde{p}\tilde{q}}(t,f)$ can be written as [5]

$$\begin{aligned} R_{pq,\tilde{p}\tilde{q}}(\Delta t, \Delta f) &= R_{pq,\tilde{p}\tilde{q}}^{SBT}(\Delta t, \Delta f) + R_{pq,\tilde{p}\tilde{q}}^{SBR}(\Delta t, \Delta f) \\ &+ R_{pq,\tilde{p}\tilde{q}}^{DB}(\Delta t, \Delta f) + R_{pq,\tilde{p}\tilde{q}}^{LoS}(\Delta t, \Delta f), \quad (2) \end{aligned}$$

where $R_{pq,\tilde{p}\tilde{q}}^{SBT}(\Delta t, \Delta f)$, $R_{pq,\tilde{p}\tilde{q}}^{SBR}(\Delta t, \Delta f)$, $R_{pq,\tilde{p}\tilde{q}}^{DB}(\Delta t, \Delta f)$, and $R_{pq,\tilde{p}\tilde{q}}^{LoS}(\Delta t, \Delta f)$ denote the normalized STF-CFs of the single-transmit, single-bounced receive, double-bounced, and LoS components, respectively, and $p, \tilde{p} \in \{1, \ldots, L_t\}$, $q, \tilde{q} \in \{1, \ldots, L_r\}$. The expressions for $R_{pq,\tilde{p}\tilde{q}}^{SBT}(\Delta t, \Delta f)$, $R_{pq,\tilde{p}\tilde{q}}^{SBR}(\Delta t, \Delta f)$, $R_{pq,\tilde{p}\tilde{q}}^{DB}(\Delta t, \Delta f)$, and $R_{pq,\tilde{p}\tilde{q}}^{LoS}(\Delta t, \Delta f)$ are given in Appendix A.

TABLE I

DEFINITION OF PARAMETERS IN FIGURE 1.

D	The distance between the centers of the Tx and Rx cylinders.
$R_t^{(l)}, R_r^{(k)}$	The radius of the l^{th} Tx and k^{th} Rx cylinder, respectively.
d_T, d_R	The spacing between two adjacent antenna elements at the Tx and Rx, respectively.
θ_T, θ_R	The orientation of the Tx and Rx antenna array in the x-y plane (relative to the *x*-axis), respectively.
ψ_T, ψ_R	The elevation of the Tx's and Rx's antenna array relative to the x-y plane, respectively.
v_T, v_R	The velocities of the Tx and Rx, respectively.
γ_T, γ_R	The moving directions of the Tx and Rx, respectively.
$\alpha_T^{(m,l)}, \alpha_T^{(n,k)}$	The azimuth angles of departure (AAoD) of the waves that impinge on the scatterers $S_T^{(m,l)}$ and $S_R^{(n,k)}$, respectively.
$\alpha_R^{(m,l)}, \alpha_R^{(n,k)}$	The azimuth angles of arrival (AAoA) of the waves scattered from $S_T^{(m,l)}$ and $S_R^{(n,k)}$, respectively.
α_R^{LoS}	The AAoA of the LoS paths.
$\beta_T^{(m,l)}, \beta_R^{(n,k)}$	The elevation angles of departure (EAoD) and the elevation angles of arrival (EAoA), respectively.
$\varepsilon_{p,m,l}$, $\varepsilon_{m,l,q}$, $\varepsilon_{p,n,k}$, $\varepsilon_{n,k,q}$, $\varepsilon_{m,l,n,k}$ and ε_{pq}	The distances $d\left(A_T^{(p)}, S_T^{(m,l)}\right)$, $d\left(S_T^{(m,l)}, A_R^{(q)}\right)$, $d\left(A_T^{(p)}, S_R^{(n,k)}\right)$, $d\left(S_T^{(m)}, S_R^{(n)}\right)$, $d\left(S_R^{(n,k)}, A_R^{(q)}\right)$, $d\left(S_T^{(m,l)}, S_R^{(n,k)}\right)$, and $d\left(A_T^{(p)}, A_R^{(q)}\right)$, respectively
h_p, h_q	The distances $d\left(O_T, O_T'\right)$ and $d\left(O_R, O_R'\right)$, respectively.

III. MAXIMUM LIKELIHOOD BASED PARAMETER ESTIMATION

The parametric nature of our wide-band channel model makes it adaptable to a variety of propagation environments. To verify our reference model with measured data, we need to estimate the model parameters from the measurements. Hence, a new maximum likelihood based stochastic estimator is derived to extract the parameters needed for our reference model from the measured data. The new estimator jointly estimates the parameters of the distribution functions used to characterize the azimuth and elevation angles of departure, the azimuth and elevation angles of arrival, and the parameters that specify how much the single- and double-bounced rays contribute to the total averaged received power, i.e., $\mathbf{\Theta} = [\beta_{T_m}, k_T, \mu_T, \beta_{R_m}, k_R, \mu_R, \eta_T, \eta_R]$. This estimator is an extension of the stochastic estimator in [10], which only estimates the parameters of the distribution function used to characterize the azimuth angles of arrival. In contrast to the estimator in [10], which estimates its parameters from the spatial correlation function, our estimator uses the STF-CF to estimate the parameters.

By observing that both the theoretical and measured input delay-spread functions are complex Gaussian random processes, we can estimate the parameters $\mathbf{\Theta} = [\beta_{T_m}, k_T, \mu_T, \beta_{R_m}, k_R, \mu_R, \eta_T, \eta_R]$ using a maximum-likelihood (ML) estimator with the log-likelihood function

$$\mathcal{L}\{\mathbf{\Theta}_{T,F}\} = -N_s\Big\{ \ln \pi^{L_r L_t} + \ln |\mathbf{R}(\mathbf{\Theta}_{T,F}, T\Delta t_s, F\Delta f_s)| + \mathrm{tr}\{\mathbf{R}(\mathbf{\Theta}_{T,F}, T\Delta t_s, F\Delta f_s)^{-1}\hat{\mathbf{R}}(T\Delta t_s, F\Delta f_s)\}\Big\}, \quad (3)$$

where $\ln(\ \cdot\ )$ denotes the natural logarithm operation, $\mathrm{tr}(\ \cdot\ )$ denotes the matrix trace, Δt_s and N_t denote the sampling period and the number of samples with respect to the time variable t, Δf_s and N_f denote the sampling period and the number of samples with respect to the frequency variable f, $N_s = N_t N_f$ is the total number of samples, $T \in \{0, \ldots, t_{\max} - 1\}$, $F \in \{0, \ldots, f_{\max} - 1\}$, $t_{\max} = \lceil 1/(B_d \Delta t_s)\rceil$, $f_{\max} = \lceil 1/(\Delta f_s \tau_{\max})\rceil$, B_d is the Doppler spread, $\tau_{\max}$ is the maximum relative delay, and $\mathbf{\Theta}_{T,F}$ denotes the vector of estimated parameters in the time and frequency instances $T\Delta t_s$ and $F\Delta f_s$[1]. The matrix $\hat{\mathbf{R}}(T\Delta t_s, F\Delta f_s)$ is the $L_t L_r \times L_t L_r$ matrix of measured correlation functions, whereas $\mathbf{R}(\mathbf{\Theta}_{T,F}, T\Delta t_s, F\Delta f_s)$ is the $L_t L_r \times L_t L_r$ matrix of theoretical correlation functions, having elements $[\mathbf{R}(\mathbf{\Theta}_{T,F}, T\Delta t_s, F\Delta f_s)]_{q+L_r(p-1),\tilde{q}+L_r(\tilde{p}-1)} = R_{pq,\tilde{p}\tilde{q}}(\mathbf{\Theta}_{T,F}, T\Delta t_s, F\Delta f_s)$ that are defined in (2). After removing the constant terms that are not dependent on the channel, the ML estimates are obtained as

$$\hat{\mathbf{\Theta}}_{T,F} = \mathrm{argmax}_{\hat{\mathbf{\Theta}}_{T,F}}\Big\{ - \ln |\mathbf{R}(\mathbf{\Theta}_{T,F}, T\Delta t_s, F\Delta f_s)| - \mathrm{tr}\{\mathbf{R}(\mathbf{\Theta}_{T,F}, T\Delta t_s, F\Delta f_s)^{-1}\hat{\mathbf{R}}(T\Delta t_s, F\Delta f_s)\}\Big\}, \quad (4)$$

with the constraint $\eta_T + \eta_R + \eta_{TR} = 1$. The expression in (4) is optimized using the sequential quadratic programming algorithm [15]. The final vector of estimated parameters $\mathbf{\Theta}$ is obtained as $\mathbf{\Theta} = (t_{\max} f_{\max})^{-1} \sum_{T=0}^{t_{\max}-1} \sum_{F=0}^{f_{\max}-1} \mathbf{\Theta}_{T,F}$.

IV. Cramér-Rao Bound

To study the performance of the proposed estimator, we derive the Cramér-Rao lower bounds (CRLB) for the estimated parameters $\mathbf{\Theta} = [\Theta_i]_{i=1}^{8} = [\beta_{T_m}, k_T, \mu_T, \beta_{R_m}, k_R, \mu_R, \eta_T, \eta_R]$. The CRLB bound of the estimated parameter Θ_i is the diagonal element of the inverse Fisher information matrix that corresponds to the parameter Θ_i. The $(i,j)^{th}$ element of the Fisher information matrix can be written as $[\mathbf{F}(\mathbf{\Theta})]_{i,j} = -\mathrm{E}\left[\partial^2\mathcal{L}(\mathbf{\Theta})/\partial\Theta_i\partial\Theta_j\right]$, where $i, j \in \{1, \ldots, 8\}$. To obtain the elements of the Fisher information matrix, we calculate the first and the second derivative of the log-likelihood function in (3) as follows:

$$\frac{\partial\mathcal{L}(\mathbf{\Theta}_{T,F})}{\partial\Theta_i} = - N_s \mathrm{tr}\Big[\Big[\mathbf{I}_{L_t L_R} - \mathbf{R}(\mathbf{\Theta}_{T,F}, T\Delta t_s, F\Delta f_s)^{-1}\hat{\mathbf{R}}(T\Delta t_s, F\Delta f_s)\Big] \times \mathbf{R}(\mathbf{\Theta}_{T,F}, T\Delta t_s, F\Delta f_s)^{-1}\mathbf{D}_{\Theta_i}(\mathbf{\Theta}_{T,F}, T\Delta t_s, F\Delta f_s)\Big], \quad (5)$$

$$\frac{\partial^2\mathcal{L}(\mathbf{\Theta}_{T,F})}{\partial\Theta_i\partial\Theta_j} = - N_s \mathrm{tr}\Big\{\mathbf{R}(\mathbf{\Theta}_{T,F}, T\Delta t_s, F\Delta f_s)^{-1}\mathbf{D}_{\Theta_j}(\mathbf{\Theta}_{T,F}, T\Delta t_s, F\Delta f_s) \times \mathbf{R}(\mathbf{\Theta}_{T,F}, T\Delta t_s, F\Delta f_s)^{-1}\hat{\mathbf{R}}(T\Delta t_s, F\Delta f_s) \times \mathbf{R}(\mathbf{\Theta}_{T,F}, T\Delta t_s, F\Delta f_s)^{-1}\mathbf{D}_{\Theta_i}(\mathbf{\Theta}_{T,F}, T\Delta t_s, F\Delta f_s) + \Big(\mathbf{I}_{L_t L_R} - \mathbf{R}(\mathbf{\Theta}_{T,F}, T\Delta t_s, F\Delta f_s)^{-1}\hat{\mathbf{R}}(T\Delta t_s, F\Delta f_s)\Big) \frac{\partial}{\partial\Theta_j}\Big[\mathbf{R}(\mathbf{\Theta}_{T,F}, T\Delta t_s, F\Delta f_s)^{-1}\mathbf{D}_{\Theta_i}(\mathbf{\Theta}_{T,F}, T\Delta t_s, F\Delta f_s)\Big]\Big\}, \quad (6)$$

$\mathbf{D}_{\Theta_i}(\mathbf{\Theta}_{T,F}, T\Delta t_s, F\Delta f_s) = \partial\mathbf{R}(\mathbf{\Theta}_{T,F}, T\Delta t_s, F\Delta f_s)/\partial\Theta_i$, $\mathbf{D}_{\Theta_j}(\mathbf{\Theta}_{T,F}, T\Delta t_s, F\Delta f_s) = \partial\mathbf{R}(\mathbf{\Theta}_{T,F}, T\Delta t_s, F\Delta f_s)/\partial\Theta_j$, and $\mathbf{I}_{L_t L_r}$ is the $L_t L_r \times L_t L_r$ identity matrix. By observing that $\mathrm{E}[\hat{\mathbf{R}}(T\Delta t_s, F\Delta f_s)] = \mathbf{R}(\mathbf{\Theta}_{T,F}, T\Delta t_s, F\Delta f_s)$, the $(i,j)^{th}$ element of the Fisher information matrix becomes

$$[\mathbf{F}(\mathbf{\Theta})]_{i,j} = -\mathrm{E}\left[\frac{\partial^2\mathcal{L}(\mathbf{\Theta})}{\partial\Theta_i\partial\Theta_j}\right] = \frac{N_s}{t_{\max} f_{\max}} \sum_{T=0}^{t_{\max}-1} \sum_{F=0}^{f_{\max}-1} \mathrm{tr}\Big\{\mathbf{R}(\mathbf{\Theta}_{T,F}, T\Delta t_s, F\Delta f_s)^{-1}\mathbf{D}_{\Theta_j}(\mathbf{\Theta}_{T,F}, T\Delta t_s, F\Delta f_s) \mathbf{R}(\mathbf{\Theta}_{T,F}, T\Delta t_s, F\Delta f_s)^{-1}\mathbf{D}_{\Theta_i}(\mathbf{\Theta}_{T,F}, T\Delta t_s, F\Delta f_s)\Big\}, \quad (7)$$

The expressions for the derivatives $\mathbf{D}_{\Theta_i}(\mathbf{\Theta}_{T,F}, T\Delta t_s, F\Delta f_s)$ can be obtained by taking the partial derivatives of the STF-CF in (2) with respect to $\Theta_{i/j}$. Here, these expressions are omitted for brevity.

V. Evaluation of the Proposed Estimator

In this section, we evaluate the performance of the proposed estimator by comparing the analytical and measured STF-CF and by comparing the mean square error of the parameter estimates to the CRLB.

To verify our reference model with measured data, we need to estimate the model parameters from the measurements. The measured data used in this paper is reported in [16]. The distances between antenna elements (d_T and d_R), the directions and speeds of the $\mathrm{T_x}$ and $\mathrm{R_x}$ (γ_T, γ_R, v_T, and v_R), the azimuth angles of the $\mathrm{T_x}$'s and $\mathrm{R_x}$'s antenna arrays (θ_T and θ_R), and the elevation angles of the $\mathrm{T_x}$'s and $\mathrm{R_x}$'s antenna arrays (ψ_T and ψ_R) are obtained from the antenna array geometry and video camera recordings. The Rice factor is estimated using the moment-method in [17]. Furthermore, the parameters R_{t2} and R_{r2} are estimated from the measured psds by setting $R_{t2} = R_{r2} = c_0\tau_{\max}/2$, where $\tau_{\max}$ is the maximum relative

[1]Operation $\lceil\cdot\rceil$ denotes rounding up to the next integer, B_d is estimated from the measured sD-psd, and $\tau_{\max}$ is estimated from the measured psds.

delay and c_0 is the speed of light. The parameters R_{t1} and R_{r1} are chosen to be $R_{t1} = R_{r1} = 0.1R_{t2}$. Finally, the parameters $\mathbf{\Theta} = [\beta_{T_m}, k_T, \mu_T, \beta_{R_m}, k_R, \mu_R, \eta_T, \eta_R]$ are estimated using the proposed maximum likelihood based stochastic estimator. Figs. 2 - 4 compare the theoretical and measured correlation functions. The parameters used to obtain curves in Figs. 2 - 4 are $\beta_{Tm} = 5.1°$, $\beta_{Rm} = 10.2°$, $\mu_T = 31.3°$, $\mu_R = 141.7°$, $k_T = 12.5$, $k_R = 10.2$, $\eta_T = 0.213$, $\eta_R = 0.234$, $\eta_{TR} = 0.553$, $\theta_T = \theta_R = 0°$, $\psi_T = \psi_R = 0°$, $\gamma_T = \gamma_R = 90°$, $\lambda = 0.123$ m, $R_{t1} = R_{r1} = 3.1$ m, $R_{t2} = R_{r2} = 31$ m, $\Delta_H = 0$, $D = 300$ m, $\gamma = 4$, $L_t = L_r = 2$, $d_T = d_R = 2.943\ \lambda$, $f_{T\max} = f_{R\max} = 90.86$ Hz, and $K = 2.41$.

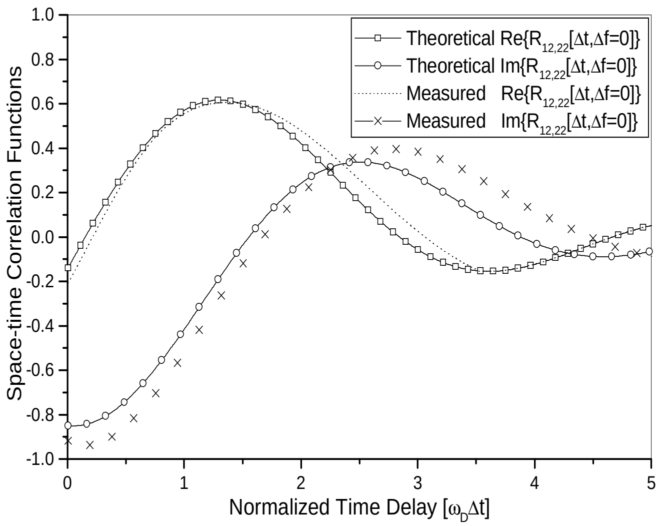

Fig. 2. Comparison of the theoretical and measured space-time correlation functions $R_{12,22}(\Delta t, \Delta f = 0)$.

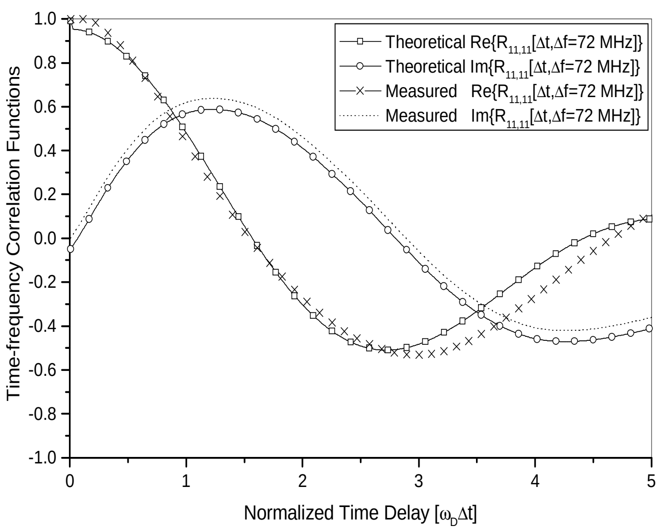

Fig. 3. Comparison of the theoretical and measured time-frequency correlation functions $R_{11,11}(\Delta t, \Delta f = 72\ \text{Hz})$.

To illustrate the performance of the proposed estimator, we compare the derived CRLB with the mean square error $\text{MSE} = (\hat{\Theta}_i - \tilde{\Theta}_i)^2$ for the parameters $[\Theta_i]_{i=1}^8 =$

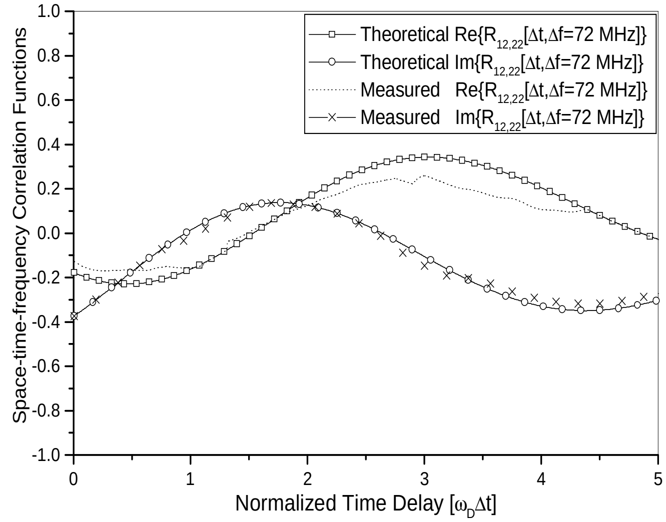

Fig. 4. Comparison of the theoretical and measured space-time-frequency correlation functions $R_{12,22}(\Delta t, \Delta f = 72\ \text{Hz})$.

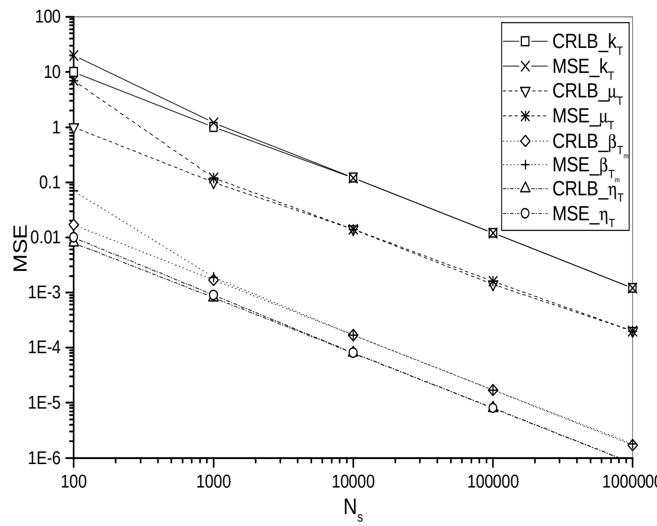

Fig. 5. Comparison of the MSE and CRLB for the parameters $[\Theta_i]_{i=1}^4 = [\beta_{T_m}, k_T, \mu_T, \eta_T]$.

$[\beta_{T_m}, k_T, \mu_T, \beta_{R_m}, k_R, \mu_R, \eta_T, \eta_R]$, where $\hat{\Theta}_i$ denotes the exact value and $\tilde{\Theta}_i$ denotes the estimated value of the parameter Θ_i. Since the results obtained for the parameters $[\beta_{R_m}, k_R, \mu_R, \eta_R]$ are almost identical with those obtained for the parameters $[\beta_{T_m}, k_T, \mu_T, \eta_T]$, Fig. 5 plots the CRLB and the MSE only for the parameters $[\Theta_i]_{i=1}^4 = [\beta_{T_m}, k_T, \mu_T, \eta_T]$. The curves in Fig. 5 are obtained with the parameters in Figs. 2 - 4. The simulation results show that the proposed estimator has asymptotically optimal performance, since it reaches the CRLB for a small number of samples, i.e., $N_s = 10^3$. The close agreement between the theoretical and empirical curves confirms the utility of the proposed estimator.

VI. Conclusions

In this paper, our 3-D reference model for wide-band MIMO M-to-M channels is reviewed. To allow comparison between the proposed model and measured data, a new maximum likelihood based stochastic estimator is derived. The proposed estimator extracts the relevant model parameters from the measured data. The performance of the new estimator is evaluated by deriving the CRLB and by comparing the mean square error of the parameter estimates to the CRLB. Simulation results show that the proposed estimator has an asymptotically optimal performance, since it reaches the CRLB for a small number of samples. Finally, the close agreement between the theoretical and empirical curves confirms the utility of the proposed estimator.

DISCLAIMER

The views and conclusions contained in this document are those of the authors and should not be interpreted as representing the official policies, either expressed or implied, of the Army Research Laboratory or the U. S. Government.

APPENDIX A
THE STF-CFS OF THE SINGLE-BOUNCED, DOUBLE-BOUNCED, AND LOS COMPONENTS

In [5] is shown that the STF-CFs of the single-bounced transmit, single-bounced receive, double-bounced, and LoS components can be closely approximated as, respectively,

$$R_{pq,\tilde{p}\tilde{q}}^{SBT}(\Delta t, \Delta f) \approx \tag{8}$$
$$\frac{\eta_T}{I_0(k_T)} \frac{\cos\left(\frac{2\pi}{\lambda}\beta_{Tm} d_{Tz}\right)}{1-\left(\frac{4\beta_{Tm} d_{Tz}}{\lambda}\right)^2} e^{-j\frac{2\pi}{\lambda}(q-\tilde{q})d_{Rx}} e^{-j2\pi\Delta t f_{R\max}\cos\gamma_R}$$
$$\int_{R_{t1}}^{R_{t2}} I_0\left(\sqrt{x_{SBT}^2+y_{SBT}^2}\right) \frac{2R_t\left(1-\gamma\frac{R_t}{D}\right)e^{-j\frac{2\pi}{c_0}\Delta f(D+R_t)}}{R_{t2}^2-R_{t1}^2} dR_t,$$
$$R_{pq,\tilde{p}\tilde{q}}^{SBR}(\Delta t, \Delta f) \approx \tag{9}$$
$$\frac{\eta_R}{I_0(k_R)} \frac{\cos\left(\frac{2\pi}{\lambda}\beta_{Rm} d_{Rz}\right)}{1-\left(\frac{4\beta_{Rm} d_{Rz}}{\lambda}\right)^2} e^{j\frac{2\pi}{\lambda}(p-\tilde{p})d_{Tx}} e^{j2\pi\Delta t f_{T\max}\cos\gamma_T}$$
$$\int_{R_{r1}}^{R_{r2}} I_0\left(\sqrt{x_{SBR}^2+y_{SBR}^2}\right) \frac{2R_r\left(1-\gamma\frac{R_r}{D}\right)e^{-j\frac{2\pi}{c_0}\Delta f(D+R_r)}}{R_{r2}^2-R_{r1}^2} dR_r,$$
$$R_{pq,\tilde{p}\tilde{q}}^{DB}(\Delta t, \Delta f) \approx \tag{10}$$
$$A_{DB}\int_{R_{t1}}^{R_{t2}} e^{-j\frac{2\pi}{c_0}\Delta f R_t} R_t I_0\left(\sqrt{x_{DB}^2+y_{DB}^2}\right) dR_t$$
$$\times \int_{R_{r1}}^{R_{r2}} e^{-j\frac{2\pi}{c_0}\Delta f R_r} R_r I_0\left(\sqrt{w_{DB}^2+z_{DB}^2}\right)\left(1-\gamma\frac{R_r}{D}\right) dR_r +$$
$$A_{DB}\int_{R_{r1}}^{R_{r2}} e^{-j\frac{2\pi}{c_0}\Delta f R_r} R_r I_0\left(\sqrt{w_{DB}^2+z_{DB}^2}\right) dR_r$$
$$\times \int_{R_{t1}}^{R_{t2}} e^{-j\frac{2\pi}{c_0}\Delta f R_t} R_t I_0\left(\sqrt{x_{DB}^2+y_{DB}^2}\right)\left(1-\gamma\frac{R_t}{D}\right) dR_t,$$
$$R_{pq,\tilde{p}\tilde{q}}^{LoS}(\Delta t, \Delta f) \approx \sqrt{K_{pq}K_{\tilde{p}\tilde{q}}}\, e^{j\frac{2\pi}{\lambda}[(p-\tilde{p})d_{Tx}-(q-\tilde{q})d_{Rx}]} \tag{11}$$
$$e^{j2\pi\Delta t[f_{T\max}\cos\gamma_T - f_{R\max}\cos\gamma_R] - \frac{2\pi}{c_0}\Delta f\sqrt{D^2+\Delta H^2}},$$

where $x_{SBT} \approx j2\pi[(p-\tilde{p})d_{Tx}/\lambda + \Delta t f_{T\max}\cos\gamma_T + \Delta f R_t/c_0] + k_T\cos\mu_T$, $y_{SBT} \approx j2\pi[(p-\tilde{p})d_{Ty}/\lambda + (q-\tilde{q})d_{Ry}\Delta_T/\lambda + \Delta t f_{T\max}\sin\gamma_T + \Delta t f_{R\max}\Delta_T\sin\gamma_R] + k_T \sin\mu_T$, $x_{SBR} \approx j2\pi[(q-\tilde{q})d_{Rx}/\lambda + \Delta t f_{R\max}\cos\gamma_R - \Delta f R_r/c_0] + k_R\cos\mu_R$, $y_{SBR} \approx j2\pi[(q-\tilde{q})d_{Ry}/\lambda + (p-\tilde{p})d_{Ty}\Delta_R/\lambda + \Delta t f_{R\max}\sin\gamma_R + \Delta t f_{T\max}\Delta_R\sin\gamma_T] + k_R \sin\mu_R$, $x_{DB} \approx j2\pi[(p-\tilde{p})d_{Tx}/\lambda + \Delta t f_{T\max}\cos\gamma_T + \Delta f R_t/c_0] + k_T\cos\mu_T$, $y_{DB} \approx j2\pi[(p-\tilde{p})d_{Ty}/\lambda + \Delta t f_{T\max}\sin\gamma_T] + k_T\sin\mu_T$, $z_{DB} \approx j2\pi[(q-\tilde{q})d_{Rx}/\lambda + \Delta t f_{R\max}\cos\gamma_R - \Delta f R_r/c_0] + k_R\cos\mu_R$, $w_{DB} \approx j2\pi[(q-\tilde{q})d_{Ry}/\lambda + \Delta t f_{R\max} \sin\gamma_R] + k_R\sin\mu_R$, $A_{DB} = \eta_{TR}\cos(2\pi\beta_{Tm}d_{Tz}/\lambda)\cos(2\pi \beta_{Rm}d_{Rz}/\lambda)2e^{-j2\pi\Delta f D/c_0}/I_0(k_T)I_0(k_R)(1-(4\beta_{Tm}d_{Tz}/\lambda)^2)(1-(4\beta_{Rm}d_{Rz}/\lambda)^2)(R_{t2}^2-R_{t1}^2)(R_{r2}^2-R_{r1}^2)$, $d_{Tz} = d_T\sin\psi_T$, $d_{Tx} = d_T\cos\psi_T\cos\theta_T$, $d_{Ty} = d_T\cos\psi_T\sin\theta_T$, $d_{Rz} = d_R\sin\psi_R$, $d_{Rx} = d_R\cos\psi_R\cos\theta_R$, $d_{Ry} = d_R\cos\psi_R\sin\theta_R$.

REFERENCES

[1] A. S. Akki and F. Haber, "A statistical model for mobile-to-mobile land communication channel," *IEEE Trans. on Veh. Tech.*, vol. 35, pp. 2–10, Feb. 1986.

[2] M. Pätzold, B. O. Hogstad, N. Youssef, and D. Kim, "A MIMO mobile-to-mobile channel model: Part I-the reference model," *Proc. IEEE PIMRC*, pp. 573–578, Berlin, Germany, Sept. 2005.

[3] A. G. Zajić and G. L. Stüber, "Space-time correlated MIMO mobile-to-mobile channels," *Proc. IEEE PIMRC*, Helsinki, Finland, Sept. 2006.

[4] A. G. Zajić and G. L. Stüber, "A three-dimensional MIMO mobile-to-mobile channel model," *IEEE WCNC*, Hong Kong, March 2007.

[5] A. G. Zajić and G. L. Stüber, "A three dimensional parametric model for wideband MIMO mobile-to-mobile channels," *Proc. IEEE GLOBECOM*, Washington, D.C., USA, Nov. 2007.

[6] K. I. Pedersen, P. E. Mogensen, and B. H. Fleury, "A stochastic model of the temporal and azimuthal dispersion seen at the base station in outdoor propagation environments," *IEEE Trans. on Veh. Tech.*, vol. 49, pp. 437–447, Mar. 2000.

[7] B. H. Fleury, P. Jourdan, and S. Stucki, "High-resolution channel parameter estimation for MIMO applications using the SAGE algorithm," *Proc. International Zurich Seminar on Broadband Communications, Access, Transmission, and Networking'02*, pp. 30-1–30-9, Feb. 2002.

[8] B. H. Fleury, M. Tschudin, R. Heddergott, D. Dahlhaus, and K. I. Pedersen, "Channel parameter estimation in mobile radio environments using the SAGE algorithm," *IEEE Journal on Selected Areas in Communications*, vol. 17, pp. 434–450, Mar. 1999.

[9] A. Abdi and M. Kaveh, "A space-time correlation model for multielement antenna systems in mobile fading channels," *IEEE J. on Select. Areas in Commun.*, vol. 20, pp. 550–560, Apr. 2002.

[10] C. B. Ribeiro, E. Ollila, and V. Koivunen, "Stochastic maximum likelihood method for propagation parameter estimation," *Proc. IEEE PIMRC*, Sept. 2004.

[11] C. B. Ribeiro, E. Ollila, and V. Koivunen, "Cram'er-Rao bound for angular propagation parameter estimation in MIMO systems," *Proc. Asilomar Conference on Signals, Systems, and Computers*, Nov. 2004.

[12] C. B. Ribeiro, E. Ollila, and V. Koivunen, "Propagation parameter estimation in MIMO systems using mixture of angular distribution model," *IEEE Int. Conf. Acoust., Speech, Signal Processing*, pp. 18–23, Philadelphia, PA, March 2005.

[13] A. Abdi, J.A. Barger, and M. Kaveh, "A parametric model for the distribution of the angle of arrival and the associated correlation function and power spectrum at the mobile station," *IEEE Trans. on Veh. Tech.*, vol. 51, pp. 425–434, May 2002.

[14] J.D. Parsons and A.M.D. Turkmani, "Characterization of mobile radio signals: model description," *IEE Proc. I, Commun., Speach, and Vision*, vol. 138, pp. 549–556, Dec. 1991.

[15] R. Fletcher, *Practical Methods of Optimization - Constrained Optimization 2e.*. John Wiley and Sons, 1981.

[16] A.G. Zajić, G.L. Stüber, Thomas G. Pratt, and Son Nguyen, "Statistical modeling with experimental verification for wideband MIMO mobile-to-mobile channels in urban environments," *Proc. ICT*, St. Petersburg, Russia, June 2008.

[17] L. J. Greenstein, D. G. Michelson, and V. Erceg, "Moment-method estimation of the Ricean K-factor," *IEEE Commun. Letters*, vol. 3, pp. 175–176, June 1999.